

# Verifying the Compton Scattering Formula and Observing the Klein-Nishina Relation

Elisa Jacquet, An Vuong, Alev Orfi

McGill University Department of Physics

Supervisor: Prof. Brunner & Prof. Sankey

April 8, 2019

## Abstract

Today, light is known to possess characteristics of both waves and particles, a property called wave-particle duality. However, in the early 1900s this was still a contested theory. In 1923, Arthur Compton famously demonstrated that the particle-nature of light was necessary to explain scattering of photons off targets. This effect is known as Compton scattering and is still one of the most well-known experiments that show evidence supporting the quantum mechanical interpretation of light as a particle. In this report, photons from a  $^{137}\text{Cs}$  source were scattered off an Al target and analysed to reproduce the results observed by Arthur Compton. We verified Compton's relation by using our data to calculate the electron's mass. It was found that the electron's mass is  $(9.4 \pm 0.3) \cdot 10^{-31}$  kg, which is in agreement with the literature value of  $m_e = (9.109\,383\,56 \pm 0.000\,000\,11) \cdot 10^{-31}$  kg. Another goal of this experiment was to verify the Klein-Nishina formula qualitatively, and thus show the importance of relativistic effects in Compton scattering. We were able to recover a linear fit between our measured counting rate and the theoretical prediction for counting rate as a function of angle. This linear relation had a  $\chi^2 = 1.5 \pm 1.0$ , supporting the Klein-Nishina formula.

# Contents

<b>1</b>	<b>Introduction</b>	<b>1</b>
<b>2</b>	<b>Experimental Set-up</b>	<b>3</b>
<b>3</b>	<b>Analysis</b>	<b>4</b>
3.1	Calibration . . . . .	4
3.2	Compton Scattering . . . . .	5
3.3	Verifying the Klein-Nishina Formula . . . . .	7
<b>4</b>	<b>Conclusion</b>	<b>10</b>

# 1 Introduction

Classically light is described as alternating electric and magnetic waves. In the twentieth century, there was an increase of experimental evidence suggesting a particle nature of light [1]. Compton scattering is among the phenomena which demonstrated the particle attributes of light [1]. This report explores the fundamental properties of Compton scattering, demonstrating experimentally the validity of this theory.

Compton scattering is the scattering of a photon off a charged particle (in this case an electron). It is found experimentally that scattered photons have longer wavelength than those incident upon the target [2]. In particular, the wavelength of the scattered light varies with the scattering angle. This shift in wavelength is described by the Compton relation [2],

$$\Delta\lambda = \frac{h}{m_e c}(1 - \cos(\theta)). \quad (1)$$

Here  $\lambda$  is the wavelength of the light,  $m_e$  is the rest mass of the electron,  $\theta$  is the scattered angle,  $h$  is Planck's constant and  $c$  is the speed of light. This formula can be expressed in terms of energy,  $E$ , using the Planck-Einstein relation,

$$E = \frac{hc}{\lambda}. \quad (2)$$

With this, the Compton relation becomes

$$\frac{1}{E_i} - \frac{1}{E_f} = \frac{1}{m_e c^2}(1 - \cos\theta). \quad (3)$$

Where  $E_f$  is the energy of the scattered photons, and  $E_i$  is the energy of the photons incident upon the electron. This change in wavelength (or energy) is explained by modelling photons as particles. The scattering can then be analyzed as an elastic collision between photons and electrons [2]. The Compton relation is retrieved by applying conservation of energy and momentum to this system. The energy of the electron after the collision is given by the relativistic energy-momentum relation [3],

$$hf + m_e c^2 = hf' + \sqrt{(p_e c)^2 + (m_e c^2)^2}. \quad (4)$$

Here  $f$  is the frequency of the light before the collision,  $f'$  is the post collision frequency and  $p_e$  is the final momentum of the electron. The conservation of momentum is a vector relation,

$$\mathbf{p}_e = \mathbf{p}_\lambda - \mathbf{p}_{\lambda'}. \quad (5)$$

Here,  $\mathbf{p}_e$  is the momentum acquired by the electron,  $\mathbf{p}_\lambda$  is the momentum of the incident photon and  $\mathbf{p}_{\lambda'}$  is the momentum of the scattered photon. Equating  $\mathbf{p}_e$  from equation 4 and equation 5 gives rise to the Compton relation [3]. As the Compton relation is a direct result of the particle nature of light, it was essential to the development of quantum physics in the early 1900s [1].

It is also of interest to define the probability that a photon will be scattered at a given angle. Mathematically, this means calculating the differential cross-section  $d\sigma/d\Omega$ . Theoretically, the differential cross-section is given by,

$$\frac{d\sigma}{d\Omega} = \frac{\text{Number of particles detected at a given angle per unit solid angle}}{\text{Number of particles incident per unit area}}. \quad (6)$$

Classically - that is without taking into account the effects of relativity - the differential cross-section is given by Thomson's formula

$$\frac{d\sigma}{d\Omega} = r_0^2 \frac{(1 + \cos^2\theta)^2}{2}. \quad (7)$$

Where  $\theta$  is the angle from the incident ray, and  $r_0 = 2.818 \times 10^{-13}$  cm is the classical radius of an electron [3]. However, for incident photons of high energy (X-ray or  $\gamma$ -ray) equation 7 no longer holds. In order to accurately describe scattering at high energy a more precise description of scattering is necessary, one which takes into account quantum mechanical and relativistic effects [3]. This description is known as the Klein-Nishina formula:

$$\frac{d\sigma}{d\Omega} = \frac{r_0^2}{2} \frac{1 + \cos^2\theta}{(1 + \alpha_0(1 - \cos\theta))^2} \left[ 1 + \frac{\alpha_0^2(1 - \cos\theta)^2}{(1 + \cos^2\theta)(1 + \alpha_0(1 - \cos\theta))} \right]. \quad (8)$$

Where  $\alpha_0 = \frac{E}{m_e c^2}$ , with  $E$  the energy of the incident photon. It is important to note here that the Thomson formula 7 is the classical limit of the Klein-Nishina formula.

This report presents an initial analysis on the phenomenon of Compton scattering. First, the quantum physical interpretation of light as a particle is verified experimentally through

the Compton relation (equation 1). Then, the importance of relativistic effects in the system is determined by demonstrating that the Klein-Nishina formula correctly models the data.

## 2 Experimental Set-up

In this experiment, a beam of photons is obtained from a 0.1 Ci source of  $^{137}\text{Cs}$ . It is known that the photons from  $^{137}\text{Cs}$  are gamma rays with energy 661.657 keV [4]. The material used to scatter these incident photons is a rod of aluminium aligned directly with the source. To detect the scattered photons, a scintillation NaI detector with a photo-multiplier is placed on a rotating disc so that the angle  $\theta$  at which scattered rays are counted can be adjusted manually. Figure 1 shows this set-up, along with the position of lead blocks used to collimate the gamma ray beam. This collimation is necessary as a safety measure and as a means to minimize background noise collected by the detector.

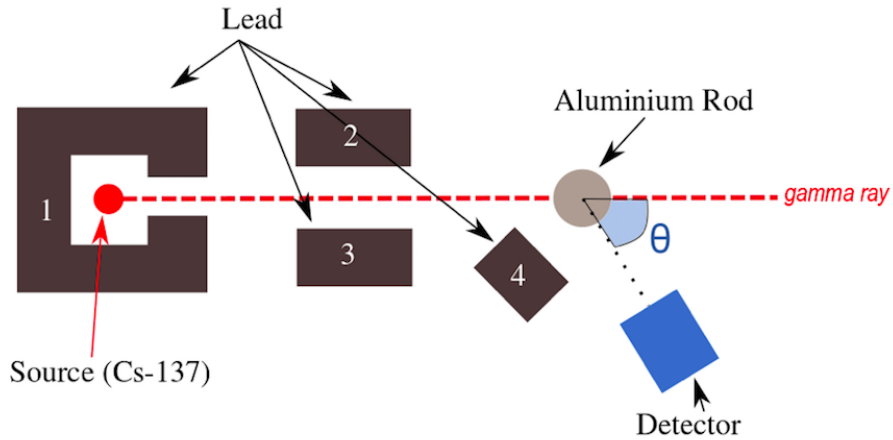


Figure 1: Experimental set-up to measure Compton scattering. Lead blocks 1-3 are used to collimate the gamma ray beam emitted from the Cs-137 source and to ensure the safety of students in the lab. Lead block 4 is positioned in such a way to minimize the detection of rays scattered by the collimators themselves (i.e. reduce background noise of detection). The angle  $\theta$  is the angle at which the scattered photons are measured and is adjusted manually.

The detector ensemble is directly connected to a computer equipped with the data-collection platform MAESTRO. Through MAESTRO, the detector can be turned on and off. The set-up gives data in the form of counts per channel. Each channel corresponds to an energy so that the measurements give the number of photons as a function of energy that are incident upon the detector at an angle  $\theta$  with respect to the incident beam. The relationship

between energy and channel number is determined in the calibration step of the experiment.

## 3 Analysis

### 3.1 Calibration

Calibration of the equipment was required to obtain the relation between channel number and energy of photons counted. This process was done by collecting three known  $\gamma$ -ray spectra from three different radioactive sources placed 10 cm from the detector:  $^{22}\text{Na}$ ,  $^{133}\text{Ba}$ , and a weaker  $^{137}\text{Cs}$ .

The spectra of these sources are well-documented such that it is known what energies the peaks in the  $\gamma$ -spectrum occur. To find a relation between energy (in keV) and channel number, it suffices to find what channel numbers each peak in the spectrum occurs at and compare this to the known energy of that peak. The energy versus channel relation is expected to be linear. Fitting this linear relationship yields the constant of proportionality between energy and channel number. This linear relationship is heavily dependent on the gain and voltage applied to the photo-multiplier/detector. For the purposes of this report, the gain will be maintained at 1.6001 and the voltage at 1000V.

A fit was performed to find the channel number of each peak. The peaks were fitted with the function described by

$$G + S + L = \left[ e^{\frac{(x-x_0)^2}{\sigma^2}} \right] + \left[ 1 - \left( 1 + e^{\frac{-(x-x_0)}{\sigma}} \right)^{-1} \right] + [mx + b] + c. \quad (9)$$

Where  $G$  is a Gaussian function centered at  $x_0$  with standard deviation  $\sigma$ ;  $S$  is a smeared step function also centered at  $x_0$ , smeared by a factor of  $\sigma$ ;  $L$  is a linear function with slope  $m$  and  $y$ -intercept  $b$ , and  $c$  represents a constant offset. The Gaussian function was used to describe the random distribution of counts about the maximum of the peak. The step function takes into account the Compton scattering that takes place within the detector's crystal, which is an intrinsic properties of detectors. Finally, the line and constant offset are included to model the background noise in the data - coming from back-scattering, scattering off the lead etc. A sample fit is shown in figure 2 where the fit was performed on the peak of  $^{137}\text{Cs}$  with energy 661.657 keV [4]. Similar fits were performed on  $^{22}\text{Na}$  with a peak at 511.0

keV [5] and  $^{133}\text{Ba}$  with peaks at 80.9979 keV [6] and 356.0129 keV [6]. The linear fit relating energy to channel number was then performed and is shown in figure 3. The conversion between channel number and energy was determined to be

$$\text{Channel Number} = (0.55622 \cdot \text{Energy}) - 4.685. \quad (10)$$

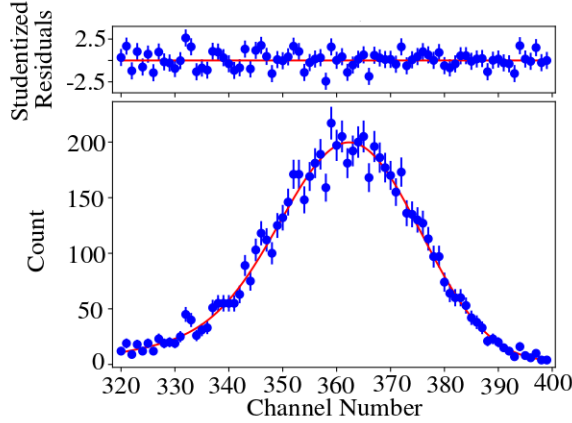


Figure 2: Sample fitting of a peak in the  $\gamma$ -ray spectrum of  $^{137}\text{Cs}$ . This is the peak corresponding to the energy value of 661.6 keV. The fit gave the peak maximum to be at channel number  $362.88 \pm 0.41$  with a  $\chi^2 = 1.04 \pm 0.16$ .

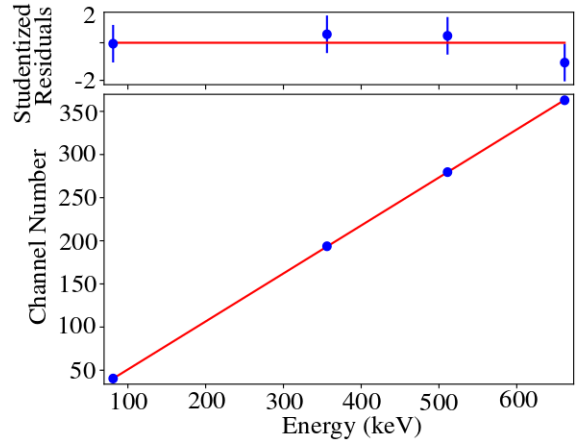


Figure 3: The plot of energy of the  $\gamma$ -rays observed versus channel number. Each point on this graph was obtained by finding the channel number of peaks in the  $\gamma$  spectra of  $^{137}\text{Cs}$ ,  $^{22}\text{Na}$ , and  $^{133}\text{Ba}$ . A linear relation is observed with slope of  $0.55622 \pm 0.00028$  and a  $y$ -intercept of  $-4.685 \pm 0.056$ , with a  $\chi^2 = 0.7 \pm 1.0$ .

### 3.2 Compton Scattering

With a relation between the bin number and the energy we can verify the Compton relation using equation 3. The energy of photons scattering off an aluminium rod was measured for 6 different angles. By the Compton relation, we show that the linear relationship between  $(1 - \cos\theta)$  and  $(\frac{1}{E_i} - \frac{1}{E_f})$ , gives slope equal to the inverse of the electron's rest energy ( $m_e c^2$ ) within uncertainty.

In order to obtain the energy of scattered photons the peaks in the measured  $\gamma$ -spectra at each angle had to be processed in a similar way as in the calibration. First, the data was processed according to calibration results to give a spectrum in terms of energy. To properly



identify the peak, a background fit was also performed: at each angle, data was collected without the Al target to observe the background radiation seen by the NaI detector. The background noise was modeled by equation 9. For each angle, this background function was fixed and added to the new fitting function in the following way:

$$G + S + \text{Background} = \left[ e^{\frac{(x-x_0)^2}{\sigma^2}} \right] + \left[ 1 - (1 + e^{\frac{-(x-x_0)}{\sigma}})^{-1} \right] + \text{Background} + c. \quad (11)$$

Here,  $G$  and  $S$  are defined in the same way as in equation 9,  $c$  is a constant offset and  $\text{Background} = G + S + L$  is a fixed function based on the data obtained without the aluminum target. With this function, it is possible to fit the peak in the observed  $\gamma$ -spectrum and get a value of the energy of the scattered ray  $E_f$ . A sample fit is shown below for  $25^\circ$ , where figure 4 shows the peak fitting in the  $\gamma$ -spectrum obtained with the aluminium target and figure 5 shows the different functions considered in the fit plotted alongside the raw data.

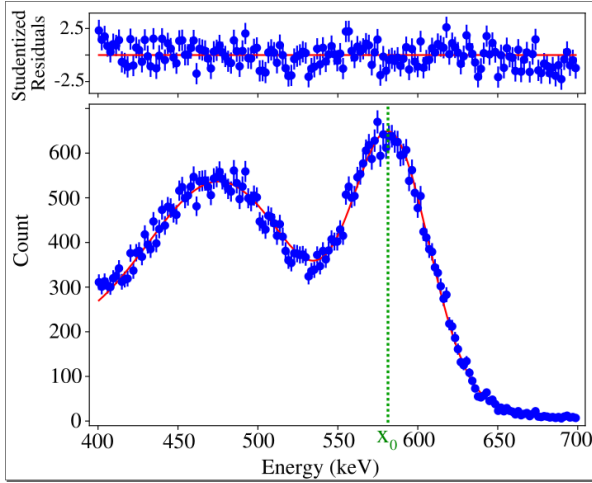


Figure 4: Sample of the fitting of the peak due to Compton scattering at  $25^\circ$ . The fit was performed with equation 9 and yielded a  $\chi^2 = 1.14 \pm 0.11$  with 162 DOF. The peak's position, shown on the figure by the green dotted line, was found to be  $x_0 = 583.65 \pm 0.26$  keV.

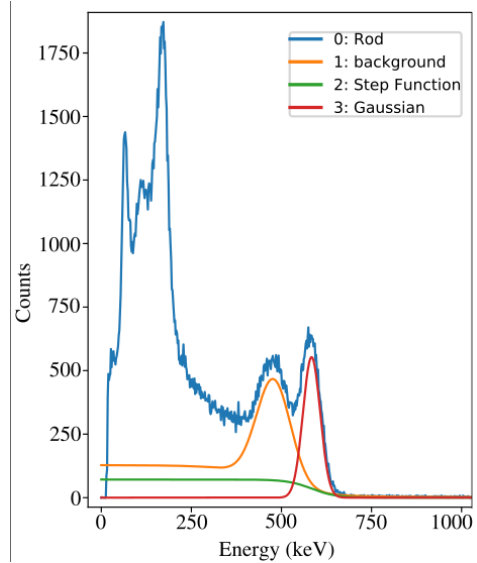


Figure 5: Four curves are shown; the raw data, the fit of the background noise, the step function characteristic of detectors, and the Gaussian curve which fits for the energy of the Compton-scattered photons.

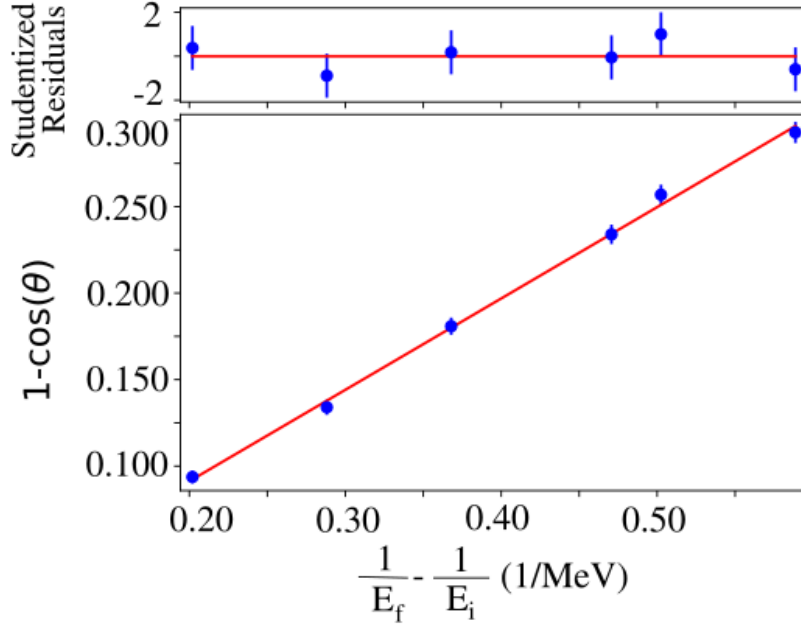


Figure 6: Experimental verification of the linear Compton relation. The slope of this line was found to be  $528.0 \pm 15.0$  keV. The fit had  $\chi^2 = 0.58 \pm 0.71$  with 4 DOF.

Using this method, the energy of photons scattered off the Al target ( $E_f$ ) was obtained for  $25^\circ$ ,  $30^\circ$ ,  $35^\circ$ ,  $40^\circ$ ,  $42^\circ$ , and  $45^\circ$ . Plotting  $(1 - \cos\theta)$  and  $(\frac{1}{E_i} - \frac{1}{E_f})$  for this data resulted in the plot shown in figure 6. Note that the function plotted is

$$m_e c^2 \left( \frac{1}{E_i} - \frac{1}{E_f} \right) = 1 - \cos\theta, \quad (12)$$

such that the slope obtained from the fit should be the rest energy of the electron. The linear fit gave a slope of  $528.0 \pm 15.0$  keV. This predicts the mass of the electron to be  $m_e = (9.4 \pm 0.3) \cdot 10^{-31}$  kg agreeing within uncertainty with the accepted value of  $m_e = (9.109\,383\,56 \pm 0.000\,000\,11) \cdot 10^{-31}$  kg [7].

### 3.3 Verifying the Klein-Nishina Formula

The Klein-Nishina Formula (equation 8) is given as a differential cross section. In this experimental setup the differential cross section is given by,

$$\frac{d\sigma}{d\Omega} = \frac{I}{(\Delta\Omega)NI_0}. \quad (13)$$

Where  $I$  is the number of scattered photons,  $N$  the number of electrons in the target,  $I_0$  the flux density at the target, and  $\Delta\Omega$  is the detector solid angle. The value of  $N$  is specific

to the material of the target and given by,

$$N = \frac{V\rho ZN_A}{M}. \quad (14)$$

Where  $V$  is the volume of the detector,  $\rho$  the material's density,  $Z$  the material's atomic number,  $M$  its molar mass, and  $N_A$  is Avogadro's number. With this relationship we have measured values for all variables in the Klein-Nishina formula excluding  $I_0$ , the flux density at the target. This value must be extrapolated through the attenuation of the beam radiation through concrete blocks. This added analysis is necessary as the detector cannot read data at  $0^\circ$  due to the high intensity of the radiation. The attenuation relation is given as

$$I = I_0 e^{-\left(\frac{\mu}{\rho}\right)x}. \quad (15)$$

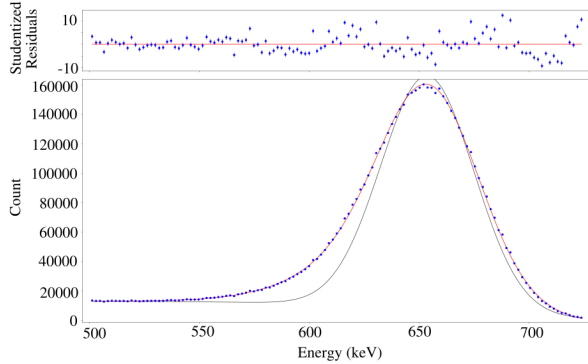


Figure 7: Sample of the fitting of the attenuation data. The fit was performed with equation 11 and yielded a  $\chi^2 = 17.35 \pm 0.13$  with 117 DOF.

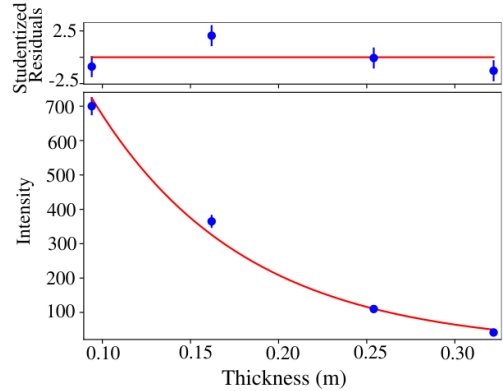


Figure 8: Exponential fit of attenuation data, yielding a  $\chi^2 = 3.3 \pm 1.0$  with 2 DOF

Where  $I$  is the measured intensity,  $x$  is the thickness of the absorbing material,  $\mu$  is the attenuation coefficient, and  $\rho$  the material's density. The value of  $\frac{\mu}{\rho}$  is known as the mass attenuation coefficient, which is  $19.7666 \pm 0.0001$  for concrete [8]. Intensity data was taken for the attenuation of the radiation through 1 to 4 concrete bricks. This data proved more difficult to analyze as we no longer had stand-alone background data and Compton scattering within the blocks added additional complexity [9]. To account for this internal scattering, a skewed Gaussian was added to our fit equation [10]. With this, we obtained the the intensity

values for the four different thicknesses of absorbing material. An example of the fit, and the corresponding fitting functions seen in figure 7.

The intensity values for each block of concrete were then fitted with an exponential function. Following equation 15 this would allow the determination of  $I_0$ . The fit is shown in figure 8. Unfortunately, the mass attenuation coefficient found with this fit is  $11.7 \pm 0.4$  which is not constant with the literature value of  $19.7666 \pm 0.0001$  [8]. This indicates an error in our data taking or fitting. Thus for the remainder of the report we will confirm the Klein-Nishina formula qualitatively as we are unable to obtain an accurate value for  $I_0$ .

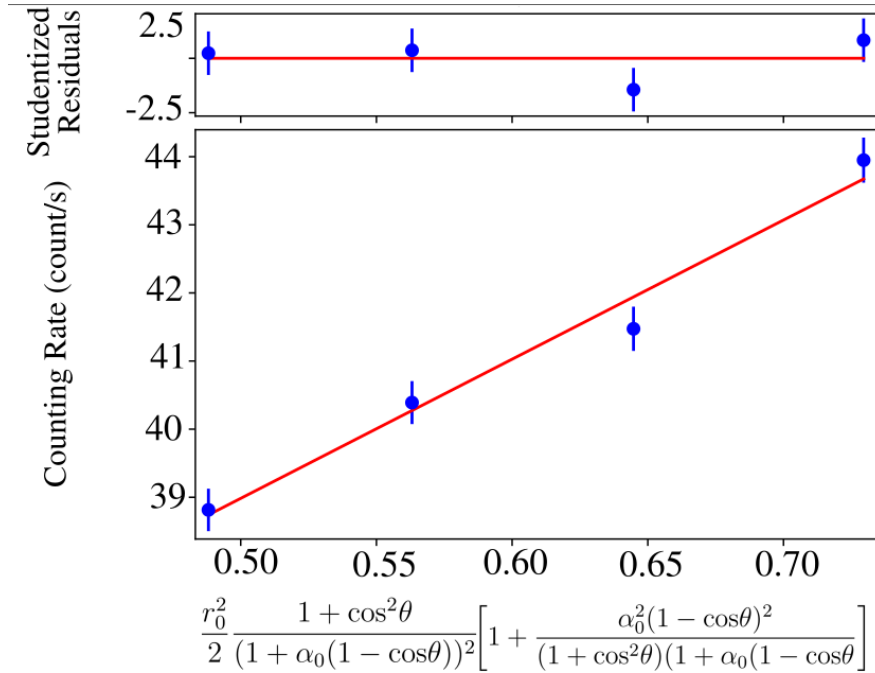


Figure 9: A linear fit of counting rate versus the value determined by the Klein-Nishina formula from the angles. A chi squared of  $1.5 \pm 1.0$  is evaluated with 2 DOF.

To verify Klein-Nishina Formula, we proceeded on calculating counting rate (number of scattered photons per unit time). This quantity is directly proportional to the differential cross-section according to equation 8. The number of counts was calculated by integrating the peak obtained by subtracting the data before and after scattering. The counting region was determined to be the full width at half the maximum of that peak. For the sake of consistency, we chose to perform this analysis on data at  $25^\circ$ ,  $30^\circ$ ,  $35^\circ$ ,  $40^\circ$ . A linear fit was used on the value determined by Klein-Nishina formula 8 from the angles and the counting rate. Figure 9 shows that a linear relation is presented, thus verifying the Klein-Nishina

formula.

## 4 Conclusion

During the twentieth century Compton scattering was one of many experiments demonstrating the particle nature of light. These experiments indicated the need for new, more general physical theories. This report demonstrates the experimental validity of the Compton relation, and thus the particle properties of light. The NaI detector was first calibrated, giving a relation between the bin number and the energy of the recorded light. This calibration was preformed by comparing the bin number and peak energy of data collected from  $^{22}\text{Na}$ ,  $^{133}\text{Ba}$ , and  $^{137}\text{Cs}$ . From there scattering data was analyzed for various angles with photons coming from a strong  $^{137}\text{Cs}$  source. Data was collected without the target allowing the background effect to be modelled. The scattered data was then fitted with the sum of the background, a Gaussian, a step function and a constant off-set, giving a peak energy for each angle. With this data a value for the relativistic mass of the electron was found using the Compton relation. Our results is within uncertainty of the literature value, showing the validity of the Compton relation.

Furthermore, we were able to able verify the Klein-Nishina formula up to a proportionality constant. This demonstrates the importance of relativistic effects in this scattering model. We showed a linear relationship between the intensity values of our data and the differential cross section given by the Klein-Nishina relation. Looking forwards, it would be important to verify the Klein-Nishina formula more formally. This would require a good measurement of  $I_0$ , the intensity of the incident beam, and would demand us to re-visit our peak-fitting model.

## References

- [1] “Arthur Compton,” *American Physical Society*, Dec 2005. [Online]. Available: <https://www.aps.org/programs/outreach/history/historicsites/compton.cfm> 1, 2
- [2] A. H. Compton, “A quantum theory of the scattering of x-rays by light elements,” *Phys. Rev.*, vol. 21, pp. 483–502, May 1923. [Online]. Available: <https://link.aps.org/doi/10.1103/PhysRev.21.483> 1
- [3] G. Gilmore, *Practical Gamma-Ray Spectrometry*, 2008. 1, 2
- [4] E. Browne, “Nuclear data sheets 108,2173,” 2007. [Online]. Available: <https://www.nndc.bnl.gov/nudat2/decaysearchdirect.jsp?nuc=137CS&unc=nds> 3, 4
- [5] M. S. Basunia, “Nuclear data sheets 127, 69,” 2015. [Online]. Available: <https://www.nndc.bnl.gov/nudat2/decaysearchdirect.jsp?nuc=22NA&unc=nds> 5
- [6] Y. Khazov, “Nuclear data sheets 112, 855,” 2011. [Online]. Available: <https://www.nndc.bnl.gov/nudat2/decaysearchdirect.jsp?nuc=133BA&unc=nds> 5
- [7] B. N. Taylor, “Fundamental constants: Electron mass,” Mar 2019. [Online]. Available: <https://physics.nist.gov/cgi-bin/cuu/Value?me> 7
- [8] S. M. Seltzer, “X-ray mass attenuation coefficients - ordinary concrete,” 2004. [Online]. Available: <https://physics.nist.gov/PhysRefData/XrayMassCoef/ComTab/concrete.html> 8, 9
- [9] R. Heath, “Computer techniques for the analysis of gamma-ray spectra obtained with nai and lithium-ion drifted germanium detectors,” *Nuclear Instruments and Methods*, vol. 43, pp. 209–229, 08 1966. 8
- [10] D. C. Radford, “Notes on the use of the program gf3,” 2000. [Online]. Available: <https://radware.phy.ornl.gov/gf3/gf3.html> 8

# Compton Scattering Lab Book

March 11/13:

- began reading through lab manual and preliminary research

Theory:

- scatter of a photon causes a change in wavelength, a decrease in energy
- this change of wavelength is dependant on the scattering angle and independant on the initial wavelength

Goals:

- demonstrate the compton effect and quantization of light
- verify the Klein-Nishinaj formula

General Info:

- it will be difficult to find  $I_0$ 
  - can find my knowing when the source was made and calculate the current  $I_0$
  - or can use an attenuation material and account for that attenuation
- Cs source, Na source and Ba source
  - use Na, Ba and weaker Cs for energy calibration
- NaI scintillation detector
  - changes incoming gamma rays to photos which are measured by PMT
  - must take the relative efficiency when comparing results at different scattering angles
  - we know how the energy changes with angle so we can use this
- given aluminium, copper and stainless steel rod
  - same energy shift but photon density is different, gamma ray mass attenuation different

Procedure:

Energy Calibration:

- obtain a spectrum for each of the calibration sources
- perform a linear fit to get the channel number/energy relation
- this sets the bias and amplifier gain

Zero Angle:

- take measurements on both sides of the zero then adjust so it is symmetric

Frequency Shift:

- used to remove background by getting data both with the target and without

Differential Cross Section:  
Measuring the Flux Density:

General Questions:

- gamma ray mass attenuation coefficient? Where does this come in? - extra?
- number of scattered photons for different rods, do we need it for comparing?
- what does the preamp do? How does changing the voltage effect data?
- Matlab function??
- is there attenuation due to the rod?

**Lab Work Schedule:**

Fri. March 15th:

- Look into the link for analysis :  
[http://www.ugrad.physics.mcgill.ca/wiki/index.php/Alpha\\_Decay#Spectrum\\_Tools](http://www.ugrad.physics.mcgill.ca/wiki/index.php/Alpha_Decay#Spectrum_Tools)
- Familiarise with computer in lab + data acquisition software

Weekend work:

- Write introduction section for report done
- Write experimental methods section
- Get better idea of what we need to do for analysis

Mon. March 18th:

- Talk to TA about functioning of equipment
- Start data collection for calibration step

Wed. March 20th:

- Finish calibration / keep up data collection

Fri. March 22nd:

- Finish calibration / keep up data collection

**Sun. March 24th: Interim Due**

- *Experimental Method Section*
  - Research on how apparatus works / background info
  - Experimental setup figure done on inkscape
  - \*should have introduction section for final report done\*
- *Analysis*
  - Calibration (included in report)
  - \*should aim to have section verifying compton relation and calculating electron rest mass done at this point\* (probably will not be included in report due to the limited space)



Background Information:

<https://www.sciencedirect.com/science/article/pii/B978141605198500006X> (section C)

To find accepted values:

- NIST (national institute of standards and technology)
- [www.nndc.bnl.gov](http://www.nndc.bnl.gov) / <https://www.nndc.bnl.gov/nudat2/>

## March 18:

Sources used for the calibration:

99 - Na22

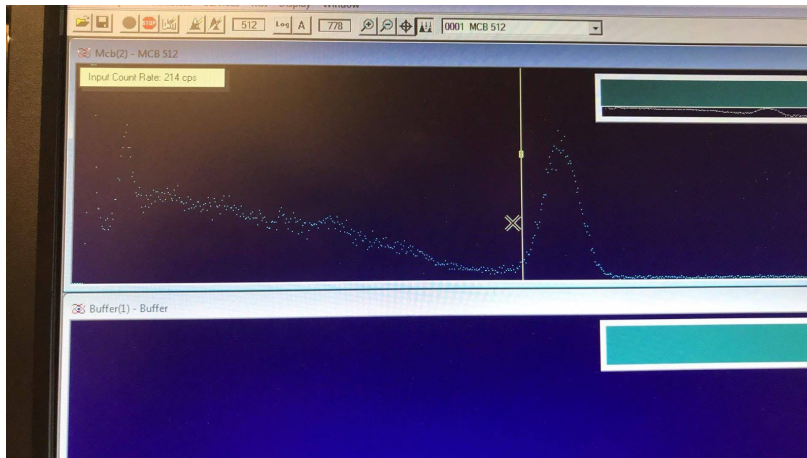
97 - Ba133

29 - Cs 137

### Calibration:

Cs 137:

Gain 1.6001 volts 1000



-can see peak

-near center so need to change gain/voltage to move it further right

-tried changing values but we found the best was 1.6001 and 1000V so will keep this throughout the lab

-ran for 180s (real) then exported data Cs137\_cali2

Ba 133:

-Gain 1.6001 volts 1000

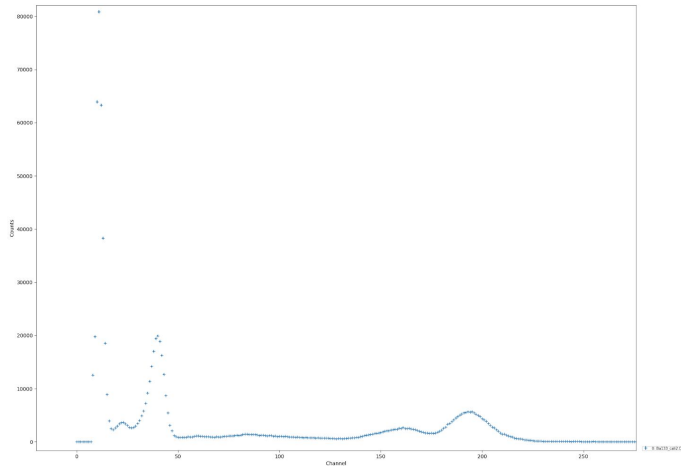
-ran for 189s (real) then exported data Ba133\_cali2

Na22:

-Gain 1.6001 volts 1000

-ran for 180s (real) then exported data Na22\_cali2

## Importing Data:

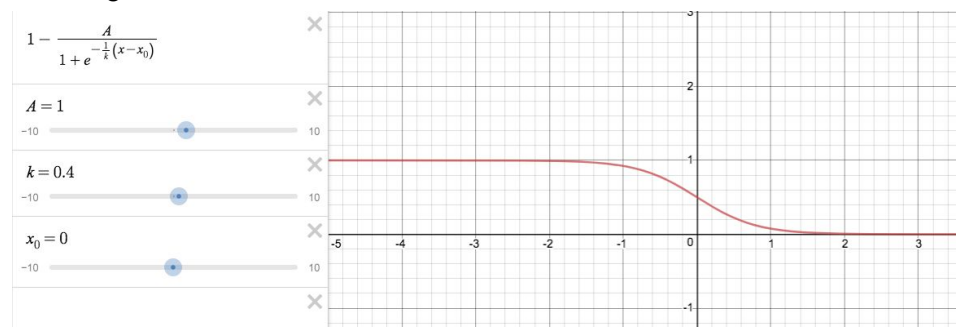


- is able to import data using Andres's code
- Ba has strong peak at 81KeV and 356KeV (lump on right)
- started to fit these with gaussians

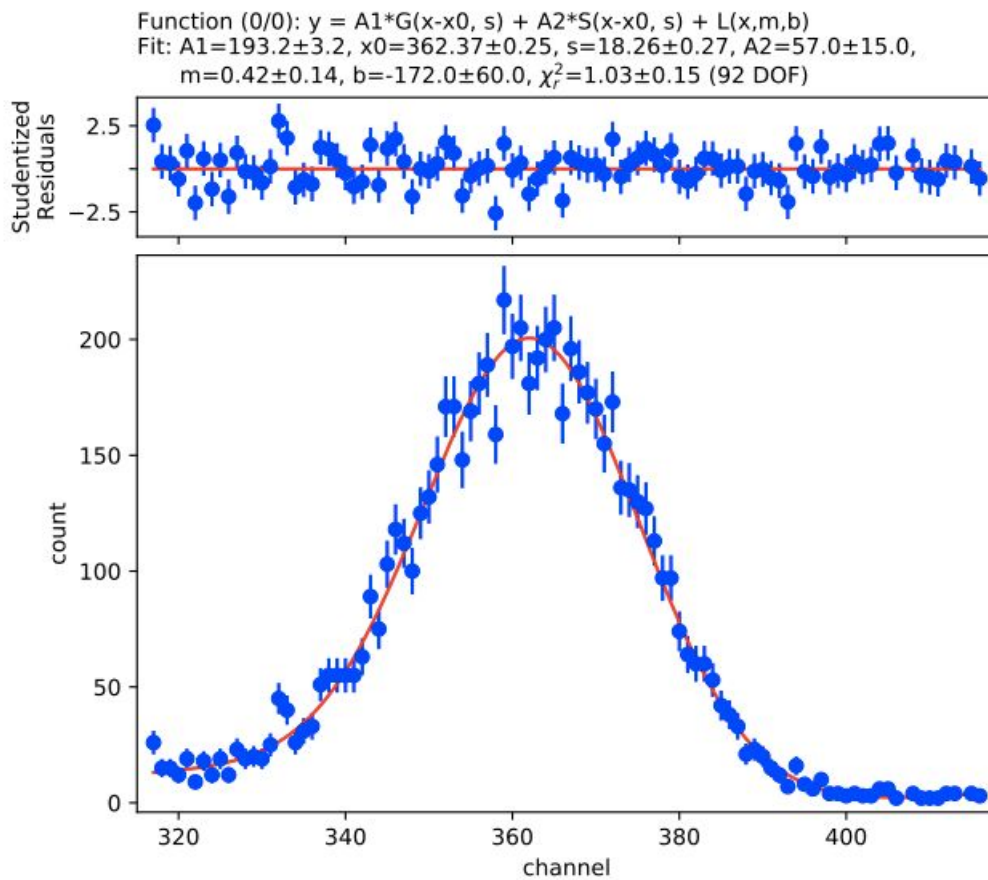
## March 20:

Fits not working well with just gaussians.

- Re-collected data for calibration by counting gamma rays from each sample for 5 min. (In the hopes of that helping get better peaks).
- Talked to TA: suggested trying to fit with double peaks.
- Talked to Prof. Brunner:
  - Explained that gaussian is not the only type of function that we need to fit to our peaks.
  - Due to the nature of the detector and scattering that happens inside the detector's crystal itself, need to also fit a smeared step function.
    - This function should be centered in the middle of gaussian peak
    - It should have the same sigma
    - Used sigmoid curve:



- Due to background noise (comes from scattering off lead, concrete, backscattering, presence of other radioactive sources etc.) also need to fit a line to the peak.
- Check on the [nndc.gov](http://nndc.gov) site for the gamma ray energies emitted by these three sources. Some have various energy rays close to one another and so some peaks may need to be fit with a double peak or quadruple peak (most for Ba133).
- This gave the following result for Cs-137 peak:





## March 25:

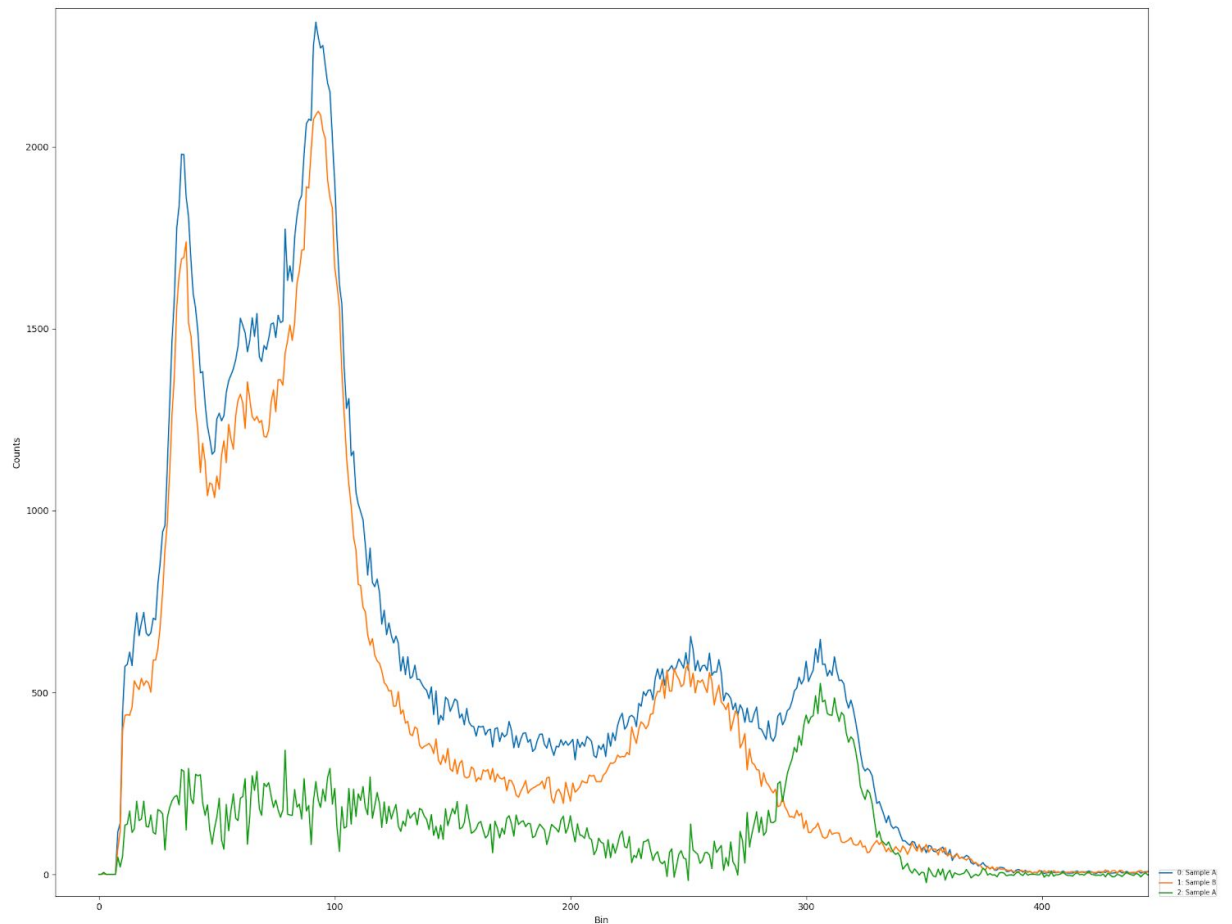
### Zero Angle Determination:

- Starting at plus 15 degrees
- 1.6001 gain 1000V 120s
- Saved at zeroangle\_15deg
- Negative 15 degrees
- 1.6001 gain 100V 120s
- Saved at zeroangle\_-15deg
- 15 deg: 371.29 +- 0.16
- -15 deg: 368.14 +- 0.54
- 

### Frequency Shift:

Aluminium rod used: OI0381

- Plus 20 degrees (110 pm 0.5)
- 1.6001 gain 1000V 400s
- Saved as 30
- Performed the same with no rod
- Saved as norod\_30
- Plus 30 degree
- 1.6001 gain 1000V 400s



- initial subtraction for 30 degrees
- Green line is subtraction of orange from blue
- Orange line is without rod, Blue is with rod

## March 27:

Aluminium rod used: OI0381

- Plus 15 degrees (105 pm 0.5)
- 1.6001 gain 1000V 400s
- Plus 25 degrees was accidentally done with stainless steel
- Plus 35 deg

## April 1:

Aluminium rod used: OI0381

- Plus 20
- 1.6001 gain 1000V 400s

- Plus 40
- 1.6001 gain 1000V 400s

Obtained measured value of  $r_{ts}$  (distance from the target to the source). It was measured to be: 53.3 cm  $\pm$  0.1 cm.

The thickness of each concrete block used was measured to be all different widths. This data was measured as part of the determination of  $I_0$ . 3 trials were conducted: 1 brick, 2 bricks, 3 bricks, 4 bricks.

TRIAL 1: The brick was measured to have a width of 9.4 cm  $\pm$  0.1

TRIAL 2: Two bricks. One of width 9.4 cm and one of width 6.8 cm.

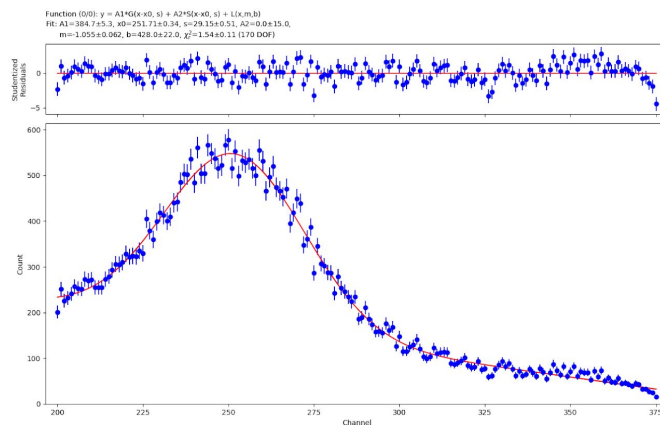
TRIAL 3: Three bricks. One of width 9.4, one of width 6.8, one of width 9.2.

TRIAL 4: Four bricks. One of width 9.4 cm, one of width 6.8, one of width 9.2, one of width 6.8.

## April 3:

Worked on fitting the scattered data

- Started by subtracting the no rod data from the rod data
- Unable to get consistent fit
  - Would change with how much data taken into account
- Tried to fit background data then keep that fit as constant and add it to scattered data fit
  - Was able to get better consistent results



Worked on fitting brick data

- Used same functions as scattered data and getting much worse chi squared
- Periodic pattern in residuals

## April 5th:

- Still having problems with fitting data for analysis on determining  $I_0$  (brick data)
- Prof. Brunner: suggested we try adding a skewed Gaussian
  - Improved the fit a lot!
  - Need to be careful with guess parameters because all the functions quickly become very strange as they try to compensate for one another.
  - *Note*: always plot all the functions against the data to make sure the fit is doing what we want it to do.
- Also improved the fit by trimming the data to the last data points and using those to fit for a linear background